

Remote RF Powering System for MEMS Strain Sensors

Nattapon Chaimanonart, Wen H. Ko, and Darrin J. Young

EECS Department, Case Western Reserve University
10900 Euclid Avenue, Cleveland, Ohio, U.S.A.
Email: nxc35@cwru.edu

Abstract

A reliable remote RF powering system is developed for industrial wireless MEMS strain sensing applications. The prototype system is insensitive to mechanical rotation and produces a stable DC voltage of 2.8 V with a 2 mA current supply capability from a 50 MHz RF power source with a power conversion efficiency of 11 %. An improved efficiency can be expected with an optimized power transmitter design. The CMOS power converter electronics are fabricated in a 1.5 μm CMOS process occupying an area of approximately 1 mm X 1 mm. The achieved DC power is adequate for supplying a high-performance wireless MEMS strain sensing system.

Keywords

Remote RF Powering, Telemetry, MEMS Sensors

INTRODUCTION

High-performance strain sensing microsystems consisting of miniature sensors and integrated interface electronics are highly critical for advanced industrial applications, such as point-stress and torque sensing for ball-bearings, rotating shafts and blades, etc. The sensed information is important for optimizing system performance, understanding material fatigue, and achieving a reliable system monitoring and intelligent control. Stringent performance requirements with a high sensitivity of 0.1 micro-strain ($\mu\epsilon$) over a wide signal bandwidth of 10 kHz and a large dynamic range of 80 dB are typically demanded for these applications. Industrial strain sensing further imposes significant design challenges due to various rotating mechanical components employed in a system. Therefore, stand-alone wireless sensing microsystems with remote powering and data telemetry capabilities are highly desirable. Inductive-coupling-based powering techniques have been widely used for biomedical implants [1-4]. In these applications, the coupling coils are fixed at certain positions with a short distance on the order of a few millimeters. It is, therefore, necessary to develop remote powering techniques, which are insensitive to mechanical rotations and can achieve an increased coupling distance for advanced industrial sensing applications. In this paper, an RF remote powering system, consisting of rotation-insensitive coupling coil loops and integrated CMOS power converter electronics, is presented to obtain a stable DC voltage of 2.8 V with a 2 mA current supply capability from a 50 MHz RF operation. The available DC power is adequate for supplying a high-performance strain sensing microsystem.

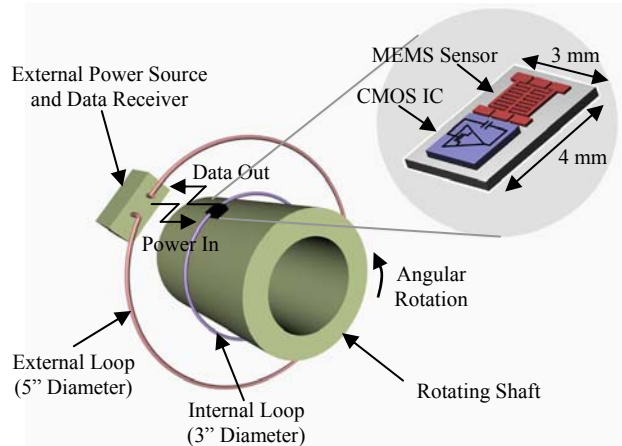


Figure 1. Wireless Microsystem Architecture

REMOTE RF POWERING ARCHITECTURE

Figure 1 presents the overall wireless microsystem architecture, which consists of an MEMS capacitive strain sensor and integrated CMOS interface and power conversion electronics, coupled with two coil loops for remote powering and data telemetry. The microsystem occupies an area of approximately 3 mm x 4 mm including package and is attached to the surface of a rotating iron shaft with a diameter of 3 inches. An internal coil is wound around the shaft and separated from the external coil by one inch for the prototype design. This configuration is critical for achieving a stable and uniform magnetic coil coupling during shaft rotation; hence a stable power conversion for supplying the wireless microsystem. The rotation of the shaft produces a rotational torque, thus a surface strain which can be sensed by the MEMS strain sensor.

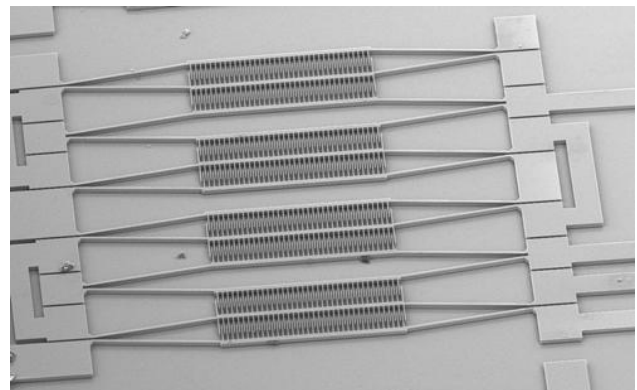


Figure 2. SEM Photo of a Fabricated Silicon MEMS Capacitive Strain Sensor

Figure 2 shows an SEM photo of a fabricated silicon MEMS capacitive strain sensor [5], which exhibits a gauge length of 1 mm and a nominal sensor capacitance value of 440 fF with a differential sensitivity of 265 aF per $\mu\epsilon$, employed for the prototype design. The sensor output can be converted to a voltage, followed by digitization and data telemetry to a nearby receiver for signal acquisition and analysis. Figure 3 presents the proposed remote RF powering architecture, where an external RF power source is used to drive a tuned series resonator consisting of L_1 and C_1 . The resistor, R_1 , represents the overall series resistance associated with the resonator including the output resistance of the power source. The resonator is tuned to an optimal frequency as will be illustrated in the following. The RF signal is coupled to a parallel resonator, consisting of L_2 and C_2 with a total loop resistance of R_2 , tuned to the same frequency. The signal is then rectified by an integrated CMOS fullwave rectifier to 5 V and further regulated to achieve a stable 3 V DC supply with a 2 mA current driving capability to power the overall microsystem as illustrated in Figure 1.

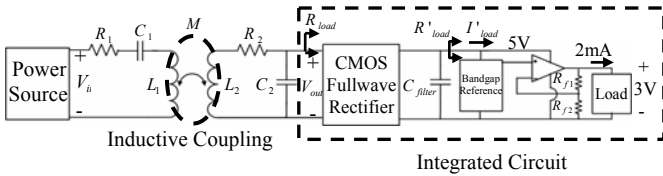


Figure 3. Remote RF Powering Architecture

In order to achieve an efficient power conversion system, the voltage gain across the tuned resonator networks needs to be maximized. The gain can be expressed as

$$V_{out} / V_{in} = \frac{\omega^2 L_2 M}{(R_1 R_2 + (\omega M)^2 + R_1 (\omega L_2)^2 / R_{load})}, \quad (1)$$

where M represents the mutual inductance between the two coil inductors: L_1 and L_2 , ω is the operating frequency, and R_{load} is the equivalent AC resistive loading presented to the parallel resonator by the CMOS fullwave rectifier, which can be determined as [6]

$$R_{load} = R'_{load} / \sqrt{2}, \quad (2)$$

where R'_{load} is the resistive loading at the fullwave rectifier output and is approximately equal to 2 k Ω due to a 2.5 mA of the loading current, I'_{load} , at the 5 V line. This then results in a resistance of 1.4 k Ω for R_{load} . In the prototype design R_1 exhibits 12 Ω , which is dominated by the output resistance of the power source. All other parameters in Equation (1), L_1 , L_2 , M , and R_2 , are a function of coil geometry, such as number of coil turns, and operating frequency. These parameters have been extensively characterized to obtain an optimal condition for achieving a maximum voltage gain. Figure 4 presents the measured voltage gain as a function of frequency and number of coil turns,

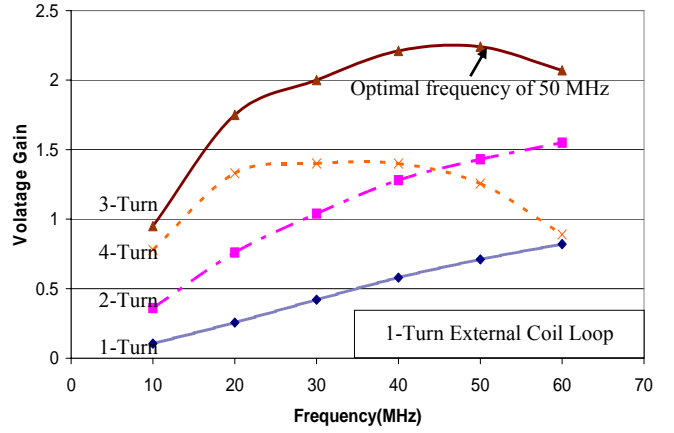


Figure 4. Measured Voltage Gain Frequency Response with Internal Coil Turn Numbers

which closely matches the predicted performance from Equation (1). It can be seen that a maximum voltage gain of 2.25 can be achieved at a 50 MHz operating frequency by employing a one-turn external coil loop, exhibiting an inductance value of 320 nH and AC resistance of 0.8 Ω , and a three-turn internal coil loop with an inductance value of 450 nH and AC resistance of 9.4 Ω . Both coil loops have self resonant frequencies well above 100 MHz and exhibit a mutual inductance of 25 nH. A design employing a four-turn internal coil loop suffers from a low voltage gain due to an excessive iron core loss at high frequencies. The one-turn external coil is chosen due to its simplicity. Furthermore, experiments have shown that a design with a two-turn external coil can achieve a comparable gain. However, a much reduced operating frequency is required, limited by the self resonant frequency of the external coil. The reduced frequency will call for an excessively large on-chip filter capacitor, as will be illustrated in the next section, to achieve a desired output voltage ripple requirement, thus unsuitable for microsystem implementation.

INTEGRATED POWER CONVERTER ELECTRONICS

An integrated CMOS fullwave rectifier is used to rectify the received RF signal. Figure 5 presents the rectifier schematic, where $V_{AC-Input}$ represents the coupled RF signal across the parallel resonator, which is to be rectified to produce a DC output voltage, $V_{DC-Output}$.

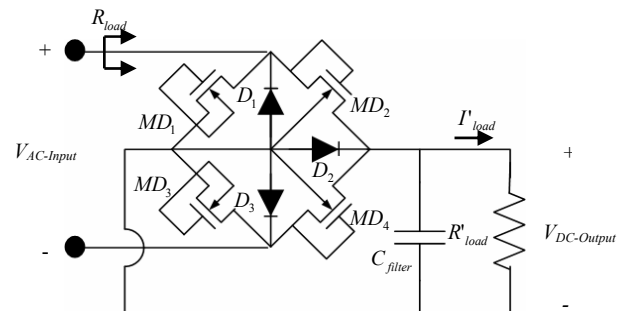


Figure 5. Simplified Inductive Coupling Circuit

The four MOSFETs connected in a diode configuration, MD_1 , MD_2 , MD_3 , and MD_4 , along with their parasitic source and drain to bulk junction diodes, D_1 , D_2 , and D_3 , form the fullwave rectifier. In a half cycle, MD_2 and D_3 perform the rectification with MD_4 and D_1 conducting during the other half cycle. The diode, D_2 , does not cause any performance degradation since it is always kept in a reverse bias condition. The total voltage drop across the rectifier is approximately 2.7 V, of which 2 V is consumed by the MOSFET diode due to an increased threshold voltage caused by body effect, and 0.7 V is dropped over the junction diode. Therefore, an RF signal with a 7.7 V amplitude is required to obtain a rectified DC output voltage of 5 V. A filtering capacitor, C_{filter} , needs to be properly selected in order to achieve a certain ripple requirement as shown in Equation (3)

$$C_{filter} = \frac{\pi \cdot I'_{load}}{V_r \omega}, \quad (3)$$

where V_r is the peak-peak ripple voltage amplitude, I'_{load} is the DC load current, and ω is the RF operating frequency. Thus, an increased operating frequency is desirable for achieving a low ripple with a reduced filtering capacitor size. The prototype wireless microsystem design specification calls for a peak-peak ripple voltage of 60 mV at the 5 V line, thus a 400 pF filtering capacitor, occupying a chip area of 0.9 mm x 0.9 mm, is required with I'_{load} of 2.5 mA.

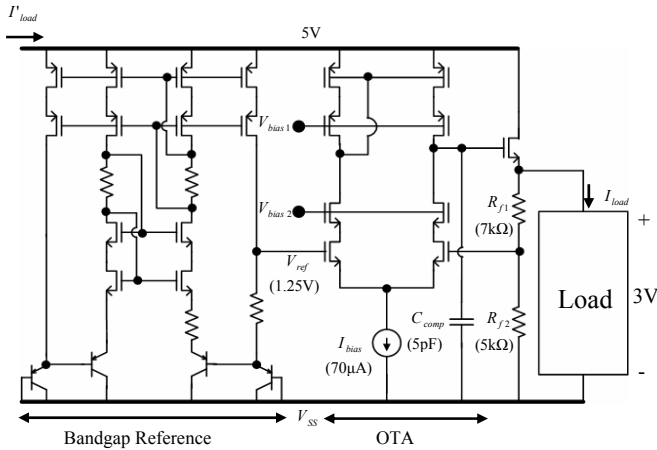


Figure 6. CMOS Linear Regulator

Figure 6 presents the schematic of a CMOS linear regulator used in the prototype system. The regulator holds the output voltage at a desired value of 3 V by comparing the output, through a resistive feedback network consisting of R_{f1} and R_{f2} , to a stable bandgap reference voltage, V_{ref} , of 1.25 V with a high-gain inverting amplifier. An OTA with a DC gain of 60 dB and unity gain frequency of 20 MHz is designed for achieving a proper regulation. Resistance values of 7 k Ω and 5 k Ω for R_{f1} and R_{f2} , respectively, are chosen to obtain a proper feedback ratio of 2.4. An output load resis-

tance of 1.5 k Ω is used throughout the design process to ensure a 2 mA current driving capability.

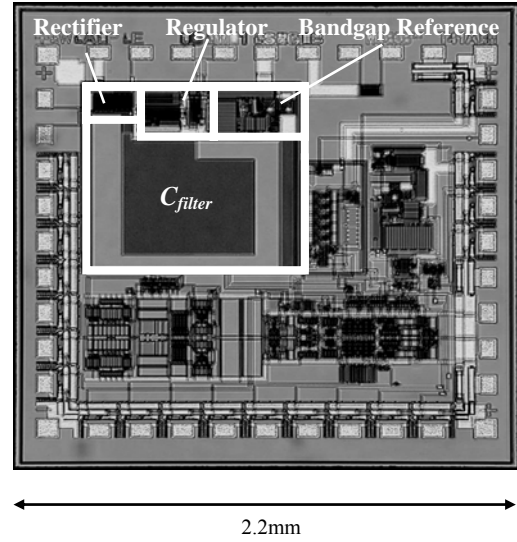


Figure 7. Chip Micrograph

MEASUREMENT RESULTS

The integrated CMOS power converter electronics are fabricated in a 1.5 μm CMOS process. Figure 7 presents the chip photo, where the converter occupies an area of approximately 1 mm x 1 mm and is also integrated with the low noise MEMS strain sensor detection electronics. The test setup for the prototype remote RF powering system is shown in Figure 8. A 50 MHz RF power source with an amplitude of 8 V peak to peak is used to drive the tuned LC network. The CMOS chip is packaged in a through-hole DIP40 package mounted on the surface of an iron shaft. The system provides a stable DC voltage of 2.8 V with a 2 mA current supply capability independent of the iron shaft rotation, thus achieving a power conversion efficiency of 11 %. An improved efficiency can be expected with an optimized power transmitter design [7]. The regulator output exhibits a line regulation and load regulation of 16 mV/V and 8 mV/mA, respectively and a ripple with an amplitude of 80 mV peak to peak. The large ripple is caused by a strong package coupling at 50 MHz, which can be substantially minimized by using an improved package. Figure 9 shows the voltage waveforms at the 5 V line and 2.8 V output. The output voltage deviates from the designed value of 3 V caused by the bandgap reference output voltage of 1.2 V due to the modeling limitation of the junction diodes used in the bandgap reference design. After completing the electrical characterization, the remote RF powering system is used to power the MEMS strain sensor and integrated low noise interface electronics to a superior performance: a minimum detectable strain of 0.09 $\mu\epsilon$ over a 10 kHz bandwidth and a dynamic range 81 dB. This is the

same performance achieved by using a 3 V power supply [8].

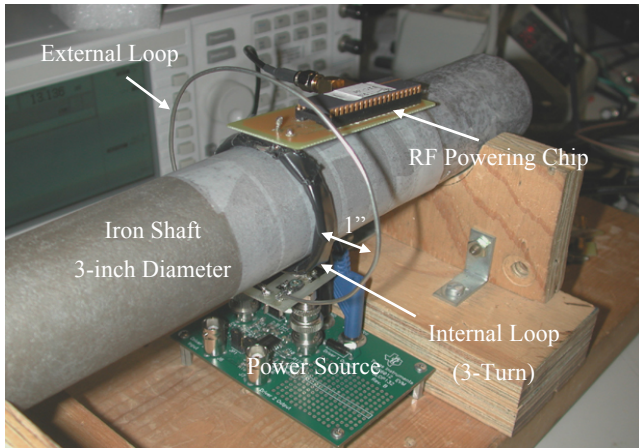


Figure 8. Test Setup

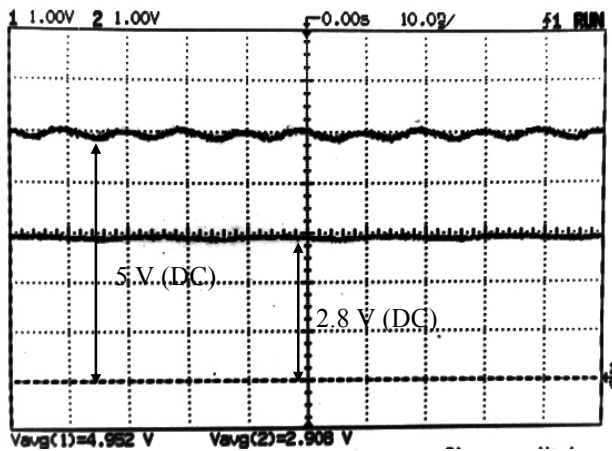


Figure 9. 5 V and 2.8 V DC Outputs

CONCLUSION

A reliable remote RF powering system for advanced industrial MEMS strain sensing application is presented. The prototype system is designed to be insensitive to mechanical rotations and outputs a stable DC voltage of 2.8 V with a 2 mA current supply capability from a 50 MHz RF operation. The power converter electronics are integrated with the low noise strain sensor interface circuitry and can pro-

vide a sufficient power to a wireless strain sensing micro-system to demonstrate a superior performance.

ACKNOWLEDGMENTS

This work is supported by U.S. Army Research Office (ARO) under contract #DADD19-02-1-0198.

REFERENCES

- [1] J. A. Von Arx and K. Najafi, "A wireless single-chip telemetry-powered neural stimulation system," *Technical Digest, IEEE International Solid-State Circuits Conference*, pp. 214 – 215, February 1999.
- [2] W. Liu and M. S. Humayun, "Retinal Prosthesis," *Technical Digest, IEEE International Solid-State Circuits Conference*, pp. 218 – 225, February 2004.
- [3] J. Ji and K. D. Wise, "An implantable CMOS circuit interface for multiplexed microelectrode recording arrays," *IEEE Journal of Solid-State Circuits*, Vol. 27, Issue 3, pp. 433 – 443, March 1992.
- [4] B. Smith, Z. Tang, M. W. Johnson, S. Pourmehdi, M. M. Gazdik, J. R. Buckett, and P. H. Peckham, "An externally powered, multichannel, implantable stimulator-telemeter for control of paralyzed muscle," *IEEE Transactions on Biomedical Engineering*, Vol. 45, Issue 4, pp. 463 – 475, April 1998.
- [5] J. Guo, H. I. Kuo, D. J. Young, and W. H. Ko, "Buckled beam linear output capacitive strain sensor," *Solid-State Sensor, Actuator and Microsystems Workshop*, pp. 344-347, June 2004.
- [6] Z. Tang, B. Smith, J. H. Schild, and P. H. Peckham, "Data transmission from an implantable biotelemetry by load-shift keying using circuit configuration modulator," *IEEE Transactions on Biomedical Engineering*, Vol. 42, No. 5, pp. 524 – 528, May 1995.
- [7] P. R. Troyk and G. A. DeMichele, "Inductively-coupled power and data link for neural prostheses using a class-E oscillator and FSK modulation," *IEEE International Conference Engineering in Medicine and Biology Society*, Vol. 4, pp. 3376 – 3379, September 2003.
- [8] M. Suster, J. Guo, N. Chaimanonart, W. H. Ko, and D. J. Young, "Low-Noise CMOS integrated sensing electronics for capacitive MEMS strain sensors," *IEEE Custom Integrated Circuits Conference*, October 2004.